

Chapter 13

An Experimental Study on Zeta Buck–Boost Converter for Application in PV System

Neeraj Priyadarshi, Kavita Yadav, Vinod Kumar and Monika Vardia

13.1 Introduction

In the present times, as fossil fuels are depleted and exhausted on large scale, eco-friendly renewable energy sources are required as an alternate source of power. Wind, solar, fuel cells, geothermal, etc. are the primary renewable energy sources. Compared to other renewable sources, the PV system is considered as an emerging renewable technology since it requires less maintenance, possess low cost, and is eco-friendly in nature [1–5]. The recent PV system has very less tracked and conversion efficiency. Therefore, maximum power point tracking (MPPT) control algorithms are required to obtain the optimal power and highly tracked efficiency. The generation of PV power depends mainly on two parameters, i.e., insolation and surrounding temperature. The MPPT algorithm enhances the tracking efficiency as well as tries to make the operating point into maximum power point (MPP) [6–10].

Several control methods are employed to obtain the peak power from the PV panel. In this paper, perturb and observe (P and O), incremental conductance, and conventional fuzzy logic controller (FLC)-based MPPT have been discussed. The main disadvantage of the above-mentioned methods is that they fail to track maximum power under changing the weather conditions as well as oscillation around MPP [11–15]. The modified FLC-based MPPT presented in this research paper works under abrupt weather conditions which has low cost and high tracking efficiency and does not require any mathematical modeling analysis.

N. Priyadarshi (✉) · K. Yadav · V. Kumar
Department of Electrical Engineering,
College of Technology and Engineering, Udaipur, India
e-mail: neerajrjd@gmail.com

M. Vardia
Faculty of Engineering, Pacific Academy of Higher Education
and Research University, Udaipur, India

In recent times, different types of DC–DC converters have attracted much attention for their potential applications in the solar energy system as an efficient MPPT tracker. Normally, these converters function as buck or boost mode. The buck–boost converter has an added advantage that they can work for both step-up or step-down operation. The buck–boost converter is used as an interface between the PV system and the grid. Among these various topologies such as four switch type, cuk, sepic, and zeta converter [16], the zeta converter is best suited for the tracking purpose mainly because it provides output voltage, which has comparatively less ripple compared to other topologies. As these converters employ binary combinations of capacitors and inductors as dynamic storage elements, they are capable of intensifying and reducing the input signal without changing the polarities. Thus, they have high efficiency, high voltage conversion ratio, low cost, and reduced voltage stress compared to other topologies of buck–boost converter.

Several control methods, namely predictive current controller [17], hysteresis current controller [18], space vector pulse-width modulation (SVPWM) [19], and space vector modulation hysteresis current controller (SVMHCC), are employed for the generation of switching signals for voltage source inverter. Compared to other existing current controller, the SVMHCC provides an enhanced and modified controlling power of the overall tracking system. The MPPT and inverter controllers are first simulated in MATLAB/Simulink and then implemented in hardware using real-time dSPACE DS1104 control board.

13.2 Topology of Proposed Photovoltaic System

Figure 13.1 shows the proposed structure of the grid-connected PV system and its control. The zeta converter performs the MPPT functions. The FLC-based controller for MPPT and SVMHCC is used to generate the gating pulses of the inverter power switches. Zeta converter works as an interface between solar panel and three-phase VSI. The real-time dSPACE DS1104 control board is employed to control the inverter and the MPPT controllers.

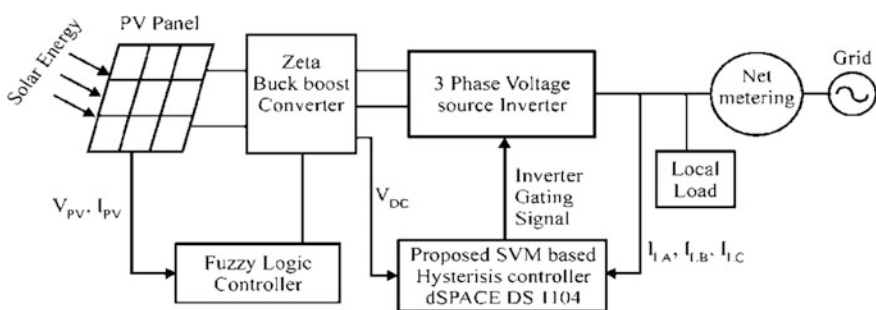


Fig. 13.1 Proposed grid PV system

13.3 Novel Control Scheme

A. Zeta Buck–Boost Converter

In the present work, the zeta converter with buck–boost characteristics has been selected, which is employed in MPPT system. The zeta converter is utilized for least output voltage ripple as a MPPT tracker. It is able to amplify and reduce the input voltage levels without inverting the polarities, as it includes two capacitors and two inductors as dynamic charge storage elements.

It has two operating modes: In the first mode, when switch is ON, the current flows through L and L_1 and diode is reversed biased, whereas the diode is forward biased in the second mode when switch is opened and inductor L_1 is fully discharged through R_L load, which is illustrated in Fig. 13.2.

B. Fuzzy Logic Controller-based MPPT

Compared to conventional MPPT algorithms, the intelligent fuzzy logic-based MPPT gives optimal tracking power, high convergence speed, and better dynamic response and there is no mathematical modeling required. It works effectively at abrupt weather condition. The block diagram of FLC, which comprises fuzzification, inference engine, and defuzzification blocks, is depicted in Fig. 13.3.

(i) Fuzzification:

Fuzzification is the method used to convert crisp value to fuzzy value. It combines the crisp input to the stored membership function which produces fuzzy inputs. The membership function is assigned for each input to convert the crisp values into fuzzy values. After assigning the membership function, it compares the stored membership function with real-time inputs to generate fuzzy inputs.

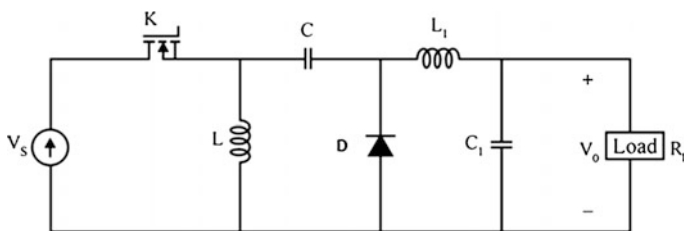


Fig. 13.2 Zeta converter

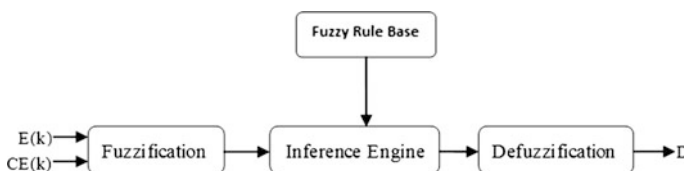


Fig. 13.3 Fuzzy logic controller

The error E and change of error CE of two fuzzy controller inputs are calculated as follows:

$$E(K) = \frac{P_{PV}(K) - P_{PV}(K - 1)}{V_{PV}(K) - V_{PV}(K - 1)} \tag{13.1}$$

$$CE(K) = E(K) - E(K - 1) \tag{13.2}$$

where $P_{PV}(K)$ and $V_{PV}(K)$ are the power and voltage of PV array, respectively. The 7 linguistic variables of input and output are shown in Fig. 13.4.

(ii) *Fuzzy inference engine (fuzzy rule base):*

The fuzzy rules are selected based on the complete behavior of the PV system. Fuzzy decisions are made on the basis of fuzzy rules to get optimal power point tracking of PV array at variable irradiance and ambient temperature. Mamdani’s method based on the max–min composition is used as a rule base, which is shown in Table 13.1.

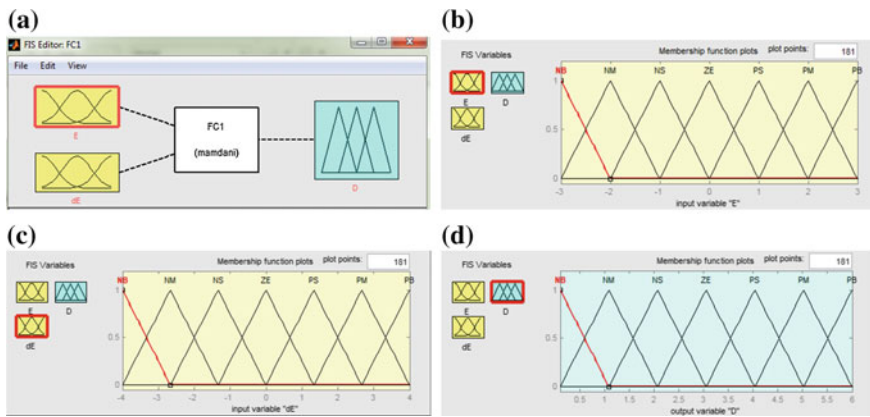
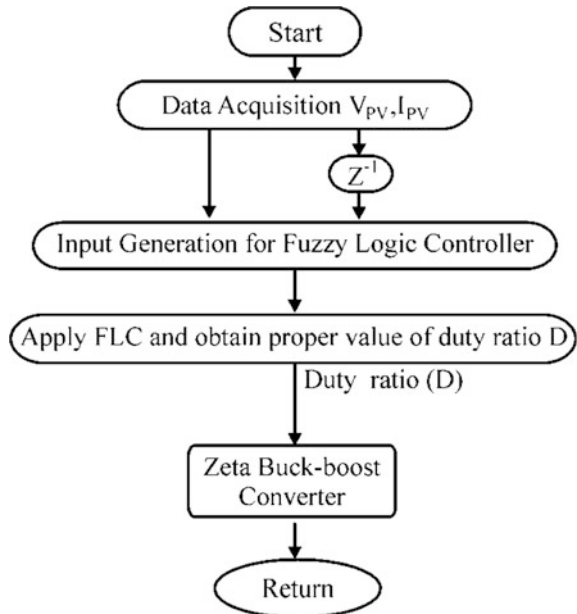


Fig. 13.4 a Picture of FLC FIS editor. b Membership function E . c Membership function dE . d Membership function output D

Table 13.1 Fuzzy rule base

dE	E						
	NB	NM	NS	ZE	PS	PM	PB
NB	ZE	ZE	ZE	PB	PB	PB	PB
NM	ZE	ZE	ZE	ZE	ZE	NM	PS
NS	ZE	ZE	PM	PS	PS	PS	PS
ZE	PS	PS	ZE	ZE	ZE	ZE	NS
PS	NS	NS	NS	NS	ZE	NS	ZE
PM	NS	NS	ZE	ZE	NS	NM	NS
PB	NB	NB	NB	NB	PM	NB	PM

Fig. 13.5 Flowchart of FLC-based MPPT algorithm



(iii) Defuzzification

Defuzzification method is used to get the numerical variable of the FLC output. The linguistic variables are converted into numerical values using this method. The defuzzification utilizes the centroid method for selecting the appropriate value of duty cycle for zeta converter. The optimum value of duty cycle is sent to the MOSFET of zeta buck–boost converter as a reference signal. The flowchart of the FLC-based MPPT is shown in Fig. 13.5.

C. Three-phase Inverter Control

Instantaneous reactive power (IRP) theory is employed to generate the reference current, which works in transient as well as in steady-state condition. Using park's transformation, the instantaneous real and reactive power is calculated. Figure 13.6 shows the complete block diagram for the generation of switching signal for three-phase voltage source inverter. This method of pulse generation is the combination of space vector modulation and hysteresis current controller. The error signal is generated by comparing the reference and actual compensating current, which works as an input to hysteresis controller. Using the switching function table, the upper and lower band errors are calculated as is shown in Fig. 13.7.

The output of upper band signal is calculated using six sectors [20] as follows:

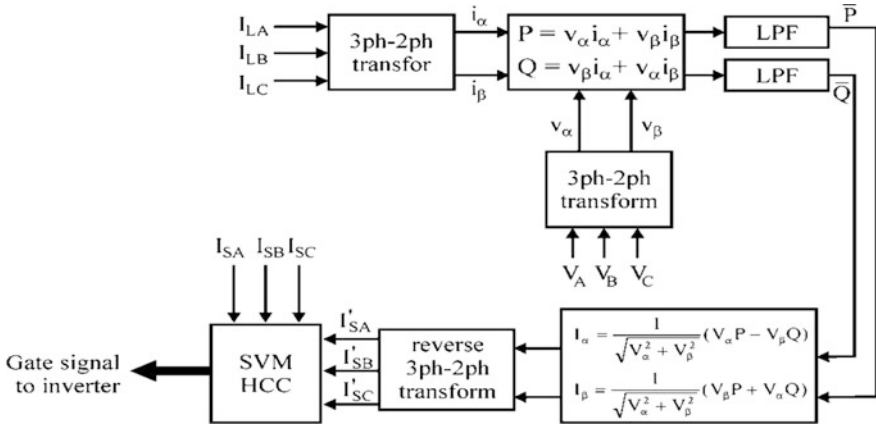


Fig. 13.6 Block diagram of three-phase VSI control

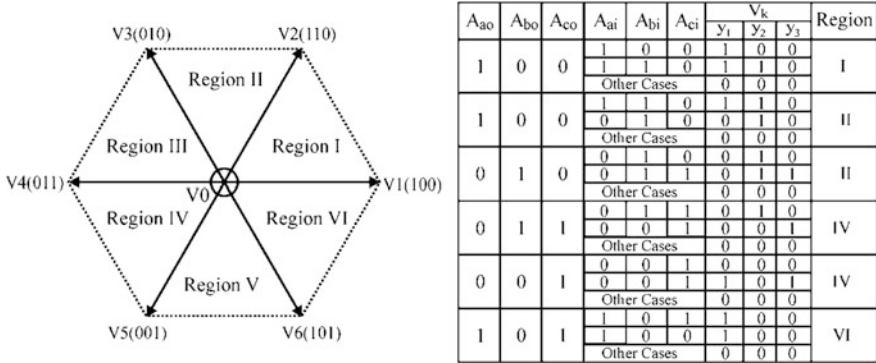


Fig. 13.7 Sectors and switching table of space vector

$$\begin{aligned}
 S_1 &= A_{ao}\bar{A}_{bo}\bar{A}_{co} \\
 S_2 &= A_{ao}A_{bo}\bar{A}_{co} \\
 S_3 &= \bar{A}_{ao}A_{bo}\bar{A}_{co} \\
 S_4 &= \bar{A}_{ao}\bar{A}_{bo}A_{co} \\
 S_5 &= \bar{A}_{ao}A_{bo}A_{co} \\
 S_6 &= A_{ao}\bar{A}_{bo}A_{co}
 \end{aligned}
 \tag{13.3}$$

where A_{ao} , A_{bo} , and A_{co} and A_{ai} , A_{bi} , and A_{ci} are upper band and lower band output hysteresis comparator signals [20].

The output of lower band signal is calculated using six sectors as follows:

$$\begin{aligned}
 y_1 &= S_1[A_{ai}\bar{A}_{bi}\bar{A}_{ci} + A_{ai}A_{bi}\bar{A}_{ci}] + S_2A_{ai}A_{bi}\bar{A}_{ci} \\
 &\quad + S_5A_{ai}\bar{A}_{bi}A_{ci} + S_6[A_{ai}\bar{A}_{bi}A_{ci} + A_{ai}\bar{A}_{bi}\bar{A}_{ci}] \\
 y_2 &= S_1A_{ai}A_{bi}\bar{A}_{ci} + S_2[A_{ai}A_{bi}\bar{A}_{ci} + \bar{A}_{ai}A_{bi}A_{ci}] \\
 &\quad + S_3[\bar{A}_{ai}A_{bi}\bar{A}_{ci} + \bar{A}_{ai}A_{bi}A_{ci}] + S_4\bar{A}_{ai}A_{bi}A_{ci} \\
 y_3 &= S_4\bar{A}_{ai}A_{bi}A_{ci} + S_4[\bar{A}_{ai}A_{bi}A_{ci} + \bar{A}_{ai}\bar{A}_{bi}A_{ci}] \\
 &\quad + S_5[\bar{A}_{ai}\bar{A}_{bi}A_{ci} + A_{ai}\bar{A}_{bi}A_{ci}] + S_6A_{ai}\bar{A}_{bi}A_{ci}
 \end{aligned}
 \tag{13.4}$$

where y_1 , y_2 , and y_3 are output signals of the inner band hysteresis comparators.

13.4 Development of Hardware Laboratory Prototype

Figure 13.8 shows the experimental setup of the proposed grid-connected PV system for performance verification. The dSPACE DS1104 kit is interfaced with Simulink-based simulation model. The voltmeter, ammeter, power quality analyzer Fluke 434, and digital oscilloscope have been used as measuring components for practical implementation. The three-phase ACs are measured using Fluke i400S. The three-phase inverter, IGBT driver, DC power supply, and pc with dSPACE DS1104 have been employed as major elements for experimental setup. Using the proposed controller, instantaneous active and reactive power, total harmonic distortion (THD), and power factor have been well maintained with better performance.

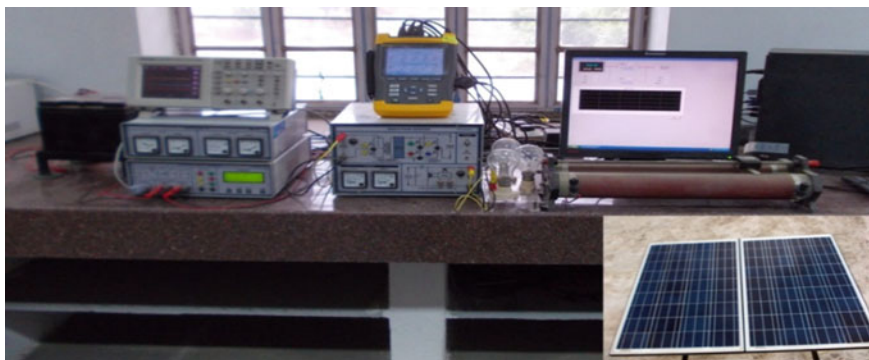


Fig. 13.8 Hardware structure of proposed grid PV system

13.5 Experimental Study Under Different Conditions

The dSPACE DS1104 kit is employed to interface with Simulink simulation model. The simulation model implemented in Simulink run on dSPACE DS1104. The PV current and voltage values are supplied to the dSPACE analog-to-digital converter and are utilized by the Simulink MPPT control block as depicted in Fig. 13.9. The generated gating pulses for three-phase VSI using dSPACE is shown in Fig. 13.10.

Figure 13.11 depicts the practical responses of grid voltage and current at unity power factor operation effectively.

By means of FLC and SVMHCC, the active and reactive power is well maintained and optimal power has been extracted through PV panel. Figure 13.12 depicts the practical responses of inverter voltage and current with fewer fluctuations.

Figure 13.13 describes the practical results of PV power, PV voltage, and PV current at steady-state condition. The PV current has low steady-state oscillation and attained MPP at relatively small time.

Figure 13.14a, b shows the THD spectrum of inverter voltage and current. The inverter voltage and current have 2.3 and 2.5% THD percentage, respectively, which follows standard IEEE 519. Figure 13.15 depicts the practical responses of PV power, PV voltage, and PV current during variable weather condition. The

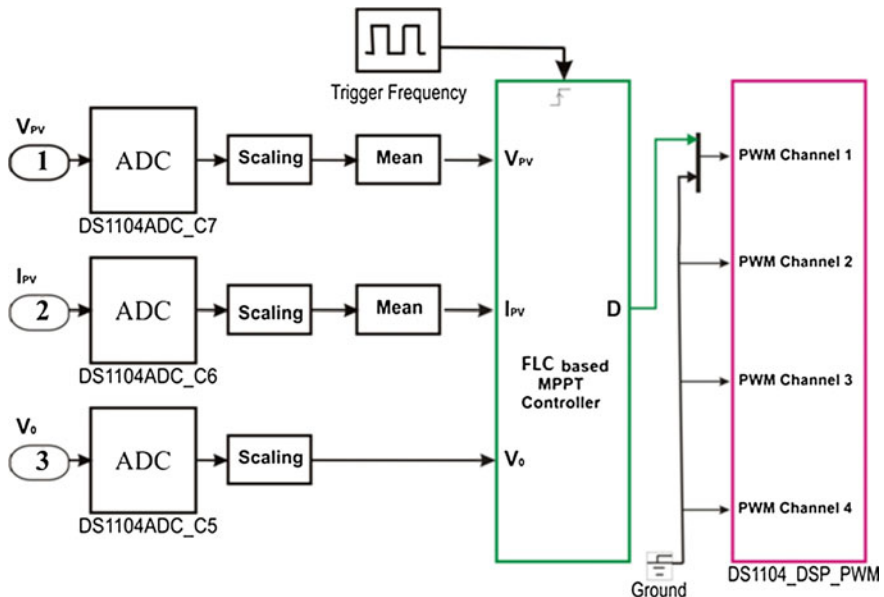


Fig. 13.9 FLC-based MPPT Simulink model for implementation in dSPACE

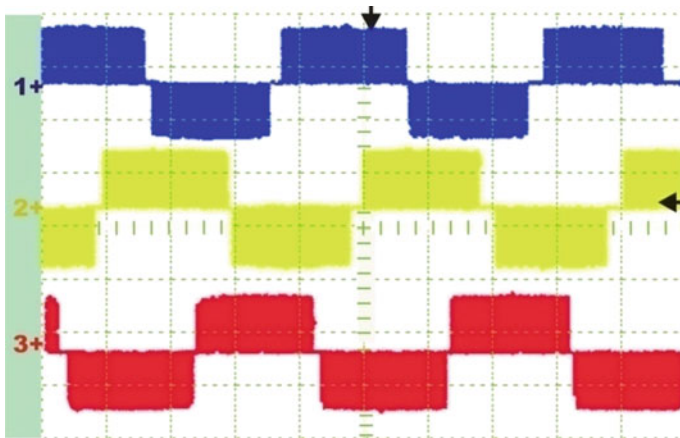


Fig. 13.10 Generated gate pulses for three-phase VSI using dSPACE

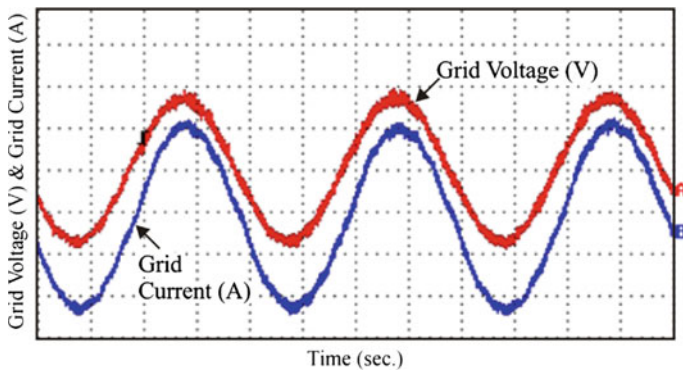


Fig. 13.11 Practical responses at unity power factor operation

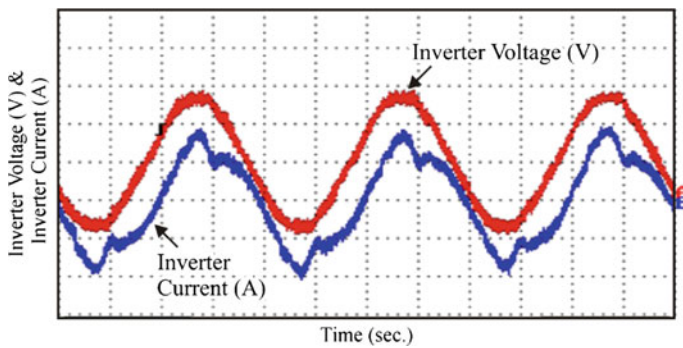


Fig. 13.12 Experimental results of inverter voltage and current

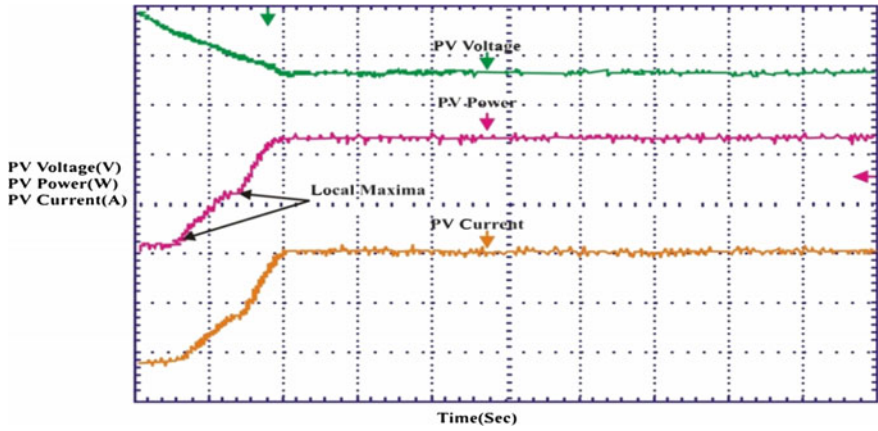
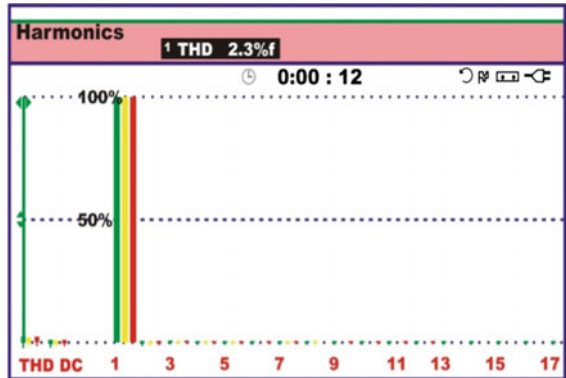
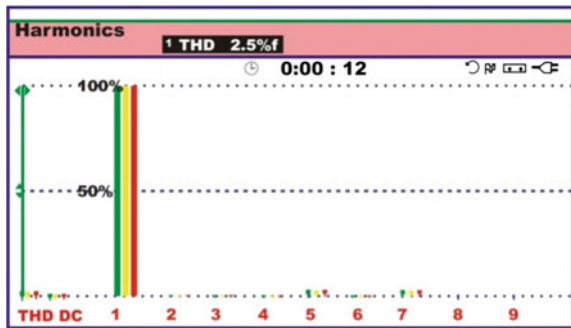


Fig. 13.13 Proposed MPPT under steady-state condition

Fig. 13.14 Total harmonic distortion spectrum



(a) Inverter voltage



(b) Inverter current

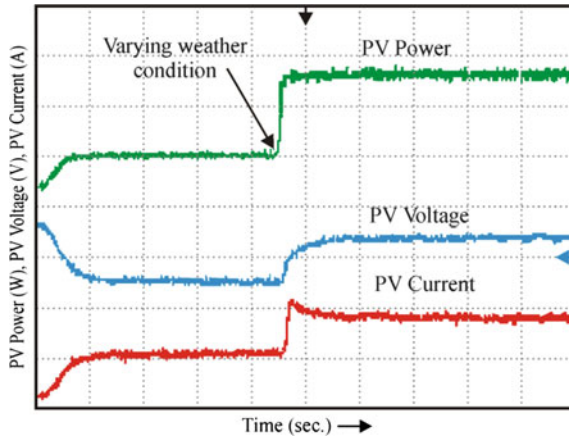


Fig. 13.15 Practical response of PV power, voltage, and current during abrupt weather condition

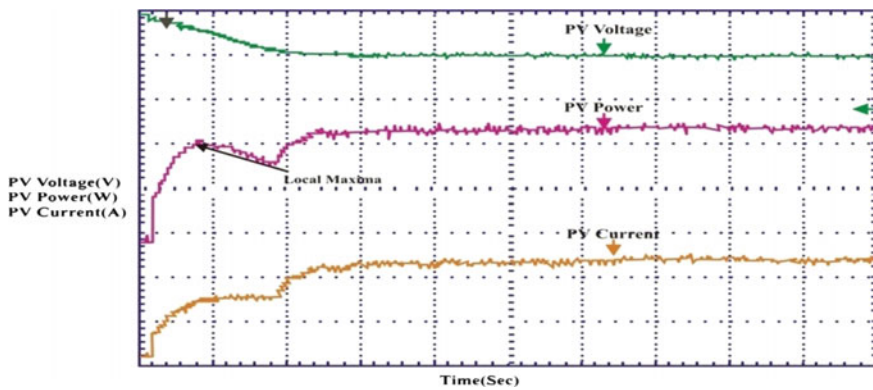
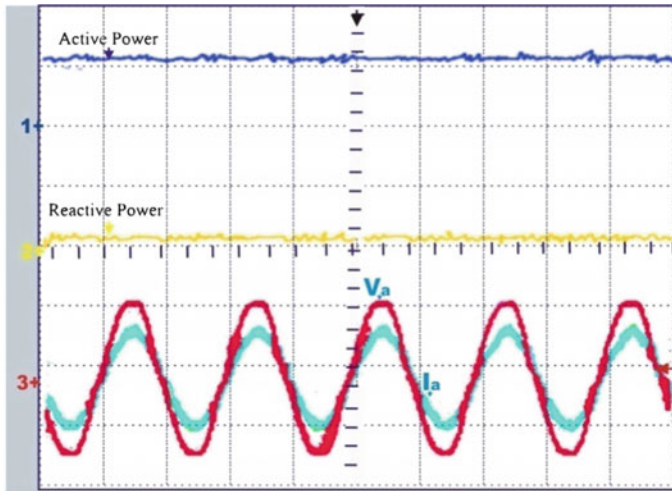


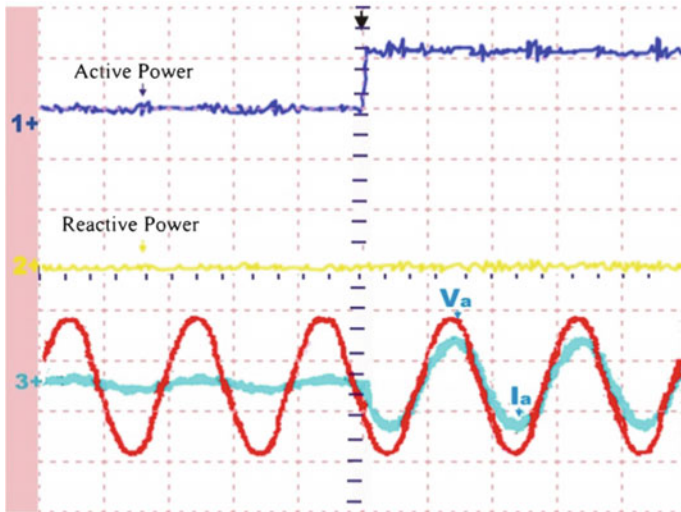
Fig. 13.16 Experimental results of the proposed MPPT under partial shading condition

proposed controller always tries to force the power to move new operating point directly under varying weather conditions. Hence, the MPP is attained in very small time and has negligible oscillation around MPP for every operating condition. To test the proposed control effectively, the PV source simulator is used to program I–V curves under partial shadow conditions. The experimental result in Fig. 13.16 shows that global MPP is achieved with small oscillation in relatively small time, which does not prevent the local maxima in the P–V curve.

Figure 13.17 shows the active and reactive power capability of the proposed grid-connected PV system. Active power is maintained constant, while the reactive power is controlled for leading, lagging, and unity power factor operation.



(a) unity power factor operation



(b) dynamic operation

Fig. 13.17 Experimental responses of active and reactive power

13.6 Conclusion

In this research work, the effectiveness of a zeta converter-based two-stage grid-integrated PV system has been investigated. The efficient control system of FLC-based MPPT and SVMHCC-based inverter control for grid-connected PV system has been implemented. For maximum power tracking and low output

voltage ripple, a zeta buck–boost converter is employed. The proposed controllers for grid-connected PV system are able to track maximum power from PV system, and it provides sinusoidal injected current to the grid in abrupt weather conditions. The hardware interface was implemented with dSPACE DS1104 real-time control board. The practical responses validate the maximum power tracking ability and stable grid requirements successfully.

References

1. Arora A, Gaur P (2015) AI based MPPT methods for grid connected PV systems under non linear changing solar irradiation. IEEE international conference on computer engineering and applications (ICACEA)-2015, pp 542–547
2. Mahmdi T, Lassad S (2015) A fuzzy controlled scheme for hybrid photovoltaic diesel AC pumping system. IEEE international conference on renewable energy congress (IREC), pp 1–6
3. Roy S (2006) Optimal planning for utility generation by photovoltaic sources spread across multiple sites. IEEE Trans Energy Convers 21(1):181–186
4. Woyte A, Van Thong V, Belmans R, Nijs J (2006) Voltage fluctuations on distribution level introduced by photovoltaic systems. IEEE Trans Energy Convers 21(1):202–209
5. Valenciaga F, Puleston PF (2005) Supervisor control for a stand-alone hybrid generation system using wind and photovoltaic energy. IEEE Trans Energy Convers 20(2):398–405
6. Billinton R (2005) Evaluation of different operating strategies in small stand-alone power systems. IEEE Transactions on energy conversion, vol 20, no 3, pp 654–660
7. Park M, Yu IK (2004) A novel real-time simulation technique of photovoltaic generation systems using RTDS. IEEE Trans Energy Convers 19(1):164–169
8. AbdulHadi M, Al-Ibrahim AM, Virk GS (2004) Neuro-fuzzy-based solar cell model. IEEE Trans Energy Convers 19(3):619–624
9. Agbossou K, Kolhe M, Hamelin J, Bose TK (2004) Performance of a stand-alone renewable energy system based on energy storage as hydrogen. IEEE Trans Energy Convers 19(3):633–640
10. Mohanty P (2014) Role of power converters in distributed solar power generation. J Autom Control Eng 2(1):38–42
11. Safari A, Mekhilef S (2011) Simulation and hardware implementation of incremental conductance MPPT with direct control method using cuk converter. IEEE Trans Ind Electron 58(4):1154–1161
12. Priyadarshi N, Kumar V, Joshi RR (2015) Zeta converter fed integrated inverter for grid connected PV system with optimal power point tracking. Int J Innov Res Sci Eng Technol 4 (2):427–433
13. El-Sayed MA, Leeb S (2015) Fuzzy logic based maximum power point tracking using boost converter for solar photovoltaic system in Kuwait. International conference on renewable energies and power quality, Spain, vol 14, no 13, April 2015
14. Reisi AR, Moradi MH (2013) Classification and comparison of maximum power point tracking techniques of photovoltaic system: Review. Renew Sustain Energy Rev 19:433–443
15. Uddin MN, Rebeiro RS (2011) Online efficiency optimization of a fuzzy-logic-controller-based IPMSM drive. IEEE Trans Ind Electron 47(2):1043–1050
16. Shiau J-K, Lee M-Y, Wei Y-C, Chen B-C (2014) Circuit simulation for solar power maximum power point tracking with different buck-boost converter topologies. Ist international e-conference on energies, pp 1–17

17. Bouafia J, Gaubert, Krim F (2010) Design and implementation of predictive current control of three-phase PWM rectifier using space-vector modulation (SVM). *Energy Convers Manag* 51:2473–2481
18. Ibrahim Z, Hasim AS, Talib N, Mustafa R (2013) Performance investigation of photovoltaic grid connection for shunt active power filter with different PWM generation. *J Theor Appl Inf Technol* 57(2):305–311
19. Chitra A, Giridharan K, Chellamuthu C (2011) Grid connected inverter with SVPWM technique for photovoltaic application. *Elixir Int J* 38:4438–4442
20. Ling LP (2004) SVM based hysteresis current controller for a three phase active power filter. University Technology, Malaysia